JET–R(99)01

P Ageladarakis et al

# Tensile and Fracture Toughness Tests of CuNiSi at Room and Cryogenic Temperatures

JET–R(99)01

# Tensile and Fracture Toughness Tests of CuNiSi at Room and Cryogenic Temperatures

P A Ageladarakis, N P O'Dowd[1], G A Webster[1].

JET Joint Undertaking, Abingdon, Oxfordshire, OX14 3EA,
[1]Imperial College, Exhibition Road, London, SW7 2BX, UK.

March 1999

“This document is intended for publication in the open literature. It is made available on the understanding that it may not be further circulated and extracts may not be published prior to publication of the original, without the consent of the Publications Officer, JET Joint Undertaking, Abingdon, Oxon, OX14 3EA, UK”.

“Enquiries about Copyright and reproduction should be addressed to the Publications Officer, JET Joint Undertaking, Abingdon, Oxon, OX14 3EA”.

## ABSTRACT

Siclanic is a copper alloy (CuNiSi) which has been extensively used at JET, the world's largest and most successful fusion device, for the fabrication of critical components. An optimised heat treatment resulted in a precipitation hardened material that exhibits much higher yield strength and electrical resistivity than similar copper alloys (e.g. CuCrZr), at a relatively wide range of temperatures, down to the ones achieved using liquid nitrogen cooling (-196$^{o}$C). Siclanic also demonstrated good mechanical formability, high thermal conductivity, as well as high adherence to vacuum deposited ceramic coatings. This material is of special interest for the design of future fusion plants. It could be a strong candidate for the primary pumps of the next-step fusion machine (ITER). An extensive experimental campaign was undertaken at Imperial College (IC), London, to quantify both the tensile and fracture behaviour of this material at temperatures of 25$^{o}$C, -80$^{o}$C and -196$^{o}$C. The tests included heat treatments and were accompanied by relevant fractographic analyses using optical and Scanning Electron Microscopes (SEM).

## 1. INTRODUCTION

A structural material able to fulfil stringent and almost conflicting requirements was sought by the JET Team, for the construction of key components at JET, namely: the liquid nitrogen (LN) screens of the Lower Hybrid Current Drive (LHCD) and divertor cryopumps (situated adjacent to and inside the main JET fusion-reaction vessel, respectively, see Figs 1,2); as well as the water cooled in-vessel baffles (20 m long, 0.3 m high, see also Fig. 2). The material had to provide high mechanical strength and electrical resistivity, to minimise the eddy current forces developed on occasions (which can reach several tonnes), and high thermal conductivity for short cooldown and warm-up periods. In addition, it had to accommodate a high density, low porosity, and flake free ceramic coating, with substantial adherence, to achieve a high emissivity (ε > 0.8) surface; this enhances the pumping capability of the LN panels (high accommodation factor), but also minimises the radiative loads to the cryopanel that they enclose (the latter is cooled by supercritical helium). Furthermore, good mechanical formability was needed, (the components of concern featured an involved geometry due to

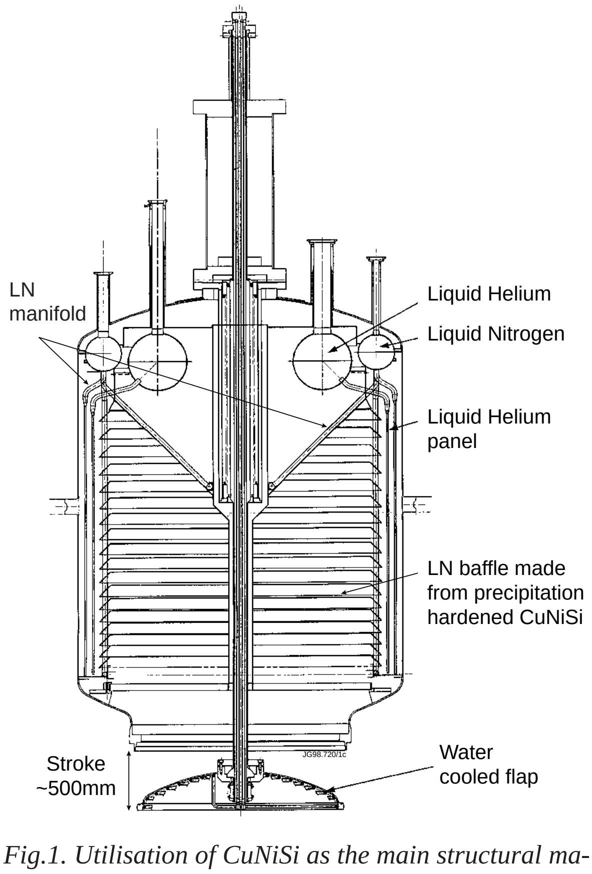


*Fig.1. Utilisation of CuNiSi as the main structural material of the LN screen of the LHCD (Lower Hybrid Current Drive) Cryopump at JET.*

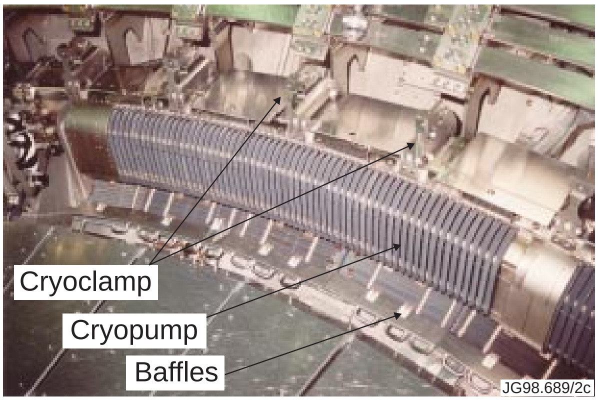


*Fig.2. Utilisation of CuNiSi for the LN chevrons of the in-vessel Cryopump and the water cooled Baffles situated at the bottom of the JET Tokamak.*

space limitations, i.e., D-profile chevrons with a V-cross section), capability of brazing on stainless steel, or inconel cooling pipes, relatively low weight, low tritium retention, radiation compatibility, low neutron activation and adequate fracture toughness. These requirements are enforced over a wide temperature range, from LN temperatures (-196$^{o}$C) up to 350$^{o}$C (during baking of the JET machine).

The material chosen for this purpose was Siclanic (initially proposed for use by L'Air Liquide, France), a copper-nickel-silicon alloy with a nominal composition of 2.5% Ni and 0.6% Si (% weight), verified also by an energy dispersing X-ray microanalysis (EDS) at Imperial College (IC), a grain size of 10 μm, and a hardness of 93 HV. During plant operation it became clear that further information, concerning the strength and fracture toughness properties of the material was needed. The scarcity of such property values in the literature concerning copper alloys and in particular for the specially heat treated Siclanic, imposed the need for a material test campaign which was undertaken at IC, to provide the above information.

## 2. PROPERTIES OF SICLANIC AND RELATED COPPER ALLOYS

Siclanic has been mainly used for electrical applications, e.g. relay springs, contact blades, conductive components, etc, offering among others, low relaxation of properties at high temperatures and excellent fatigue resistance [1]. The physical properties of Siclanic are shown in Table 1. However this material has never been used as a main cryopump structural material.

The primary requirements for the material of the JET components were; (a) electrical resistivity higher than 2E-6 Ω cm, (b) thermal conductivity higher than 1 W/cm$^{o}$C and (c) yield strength higher than 200 MPa, for a temperature range -196$^{o}$C to 350$^{o}$C.

The need for high thermal conductivity is primarily met by copper and some of its alloys, such as [2-4] the high purity copper (99.999%, or coalesced 99.98%), oxygen free copper (99.95% pure annealed),Cu+1% Pb, or Cu+0.6 Te, CuCrZr and Siclanic. Other metals (eg, Fe, Ni, Cr, Stainless Steel), or even some copper alloys [4], e.g., Beryllium Copper (2% Be), Silicon Bronze (3.15% Si, 13%Mn, 1% Zn), Phosphorus Copper (0.027% P), Brass, etc., exhibit much lower thermal conductivity (by a factor of two in some cases) especially at cryogenic temperatures, although their electrical resistivity is higher than the desired value. The latter is an expected tendency since materials with high electrical resistivity normally exhibit high thermal resistivity as well. A number of copper alloys were reviewed, (ie copper alloyed with Al, Fe, Mn, Ni, Pb, Sn, Zn in various compositions and combinations), but their properties of concern could not

*Table 1. Physical Properties of CuNiSi including different metallurgical conditions*

| Specific Heat [J/g° C] | Mass per Unit Volume [g/cm$^3$] | Melting Range [° C] | Linear Expansion Coefficient |
|---|---|---|---|
| 0.37 | 8.9 | 1040– 1060 | 19.E-6 (20– 300° C) |
| | Thermal Conductivity [W/m° C] | Electrical Resistivity µ cm] | Modulus of Elasticity [GPa] |
| Solid Solution | 84 (20° C) | 7.8 (20° C) | 120 (20° C) |
| Optimised Preception Hardened | 220 (20° C)<br>85 (-196° C) | 4.6 (20° C)<br>2.9 (-196° C) | 125 (20° C)<br>129 (-196° C) |

meet all the imposed requirements, at the same time [5]. The additional need for a relatively high tensile strength (higher than 200 MPa) over a range which covers cryogenic temperatures, reduced the candidate materials to CuCrZr and Siclanic.

Prior to the construction of components (1990) the JET Team conducted a preliminary experimental campaign to obtain the property values of these two materials at the respective temperature range. The measurements were performed in collaboration with Riso, Denmark and the results are given in Table 2. High strength was achieved after an optimisation of a precipitation treatment [6]. It may be seen that CuNiSi was superior to CuCrZr since it provided higher yield strength (ranging from 420 to 460 MPa instead of 298 to 306 MPa) and higher electrical resistivity (from 4.6 to 2.9E-6 Ω cm instead of 0.7 to 2.42E-6 Ω cm), and therefore it was chosen

*Table 2. Comparison of mechanical properties of CuNiSi and CuCrZr at different temperatures.*

| **Material** | **Property** | **Temperature** | **Result** |
|---|---|---|---|
| CuCrZr | Thermal Conductivity W cm$^{-1}$ K$^{-1}$ | 20 | 3.5 |
| CuNiSi | | 20 | 2.2 |
| | | -196 | 0.85 |
| CuCrZr | Electrical Resistivity µ cm | 20 | 2.42 |
| | | -196 | 0.70 |
| CuNiSi | | 20 | 4.6 |
| | | -196 | 2.9 |
| CuCrZr | 0.2% Strength MPa | 20 | 298 |
| | | -196 | 306 |
| CuNiSi | | 20 | 426 |
| | | -196 | 460 |

for the construction of the cryopump system components. Two additional characteristics favoured Siclanic over CuCrZr; the significantly lower cost of the former, as well as its availability in thin sheet forms, required for the construction of the components concerned.

## 3. HEAT TREATMENT OF SICLANIC SPECIMENS

Tensile and Compact Tension (CT) specimens were cut from a flat rolled thin rectangular sheet (2m x 0.5m x 3mm), provided by MSX-Clal, France, (the manufacturer of the JET components), in a TB-Trempé or "W" state [7], meaning a material which has been solution treated (at 800$^o$C-810$^o$C), water quenched and responsive to precipitation treatment. The manufacturing process has a limited cooling capacity for it is concerned primarily with the production of CuNiSi for electrical/electronic applications, where thin sheets (up to 3 mm) are required. Therefore, only specimens with a relatively small thickness, were available. However, it should be pointed out that this was the thickness of the components used in the JET apparatus. The specimens were cut according to the specifications of the relevant standards [8-10] and are shown in Fig. 3.

CuNiSi is offered by the manufacturer in two categories of metallurgical condition, in particular, solution treated and cold worked, or solution treated and precipitation hardened. The latter, together with the spinodal-decomposition type, cover most of the commercial copper alloys. These treatments rely on the decomposition of a supersaturated solid solution at an elevated temperature to produce homogeneous precipitation of a second phase ($Ni_2Si$ for Siclanic) on a very fine scale with particles in the size range from 1 nm$^3$ to 10 nm$^3$.

The properties required from the Siclanic however, were only achieved after an optimisation of a precipitation hardening process, (see Fig 4), that consists of a solution treatment (up to

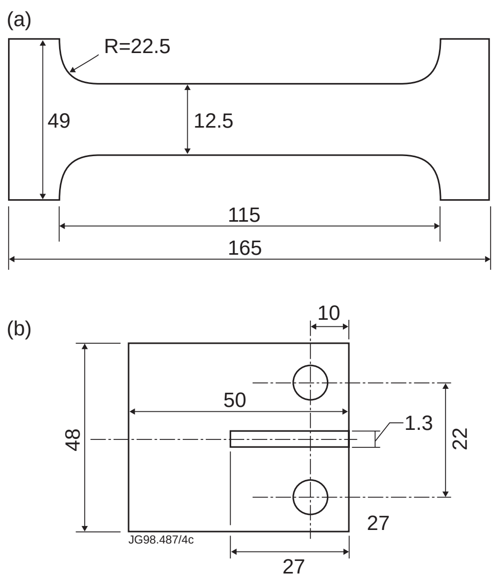


*Fig.3. Flat thin sheet Tensile and Compact Tension (CT) specimens used throughout the experimental campaign.*

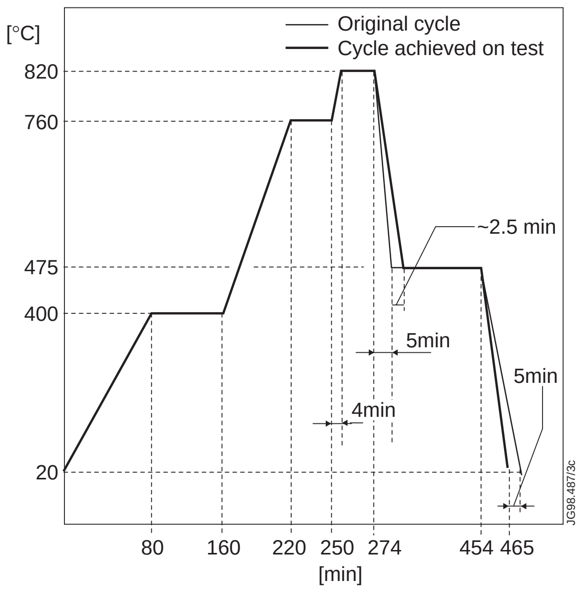


*Fig.4. Optimised precipitation hardening treatment applied to solution (as-received) CuNiSi specimens. The cycle consists of a solution treatment at 820$^o$C and an age hardening process at 475$^o$C.*

820°C) and an aged-hardening process at 475°C. Fig 4 depicts both the heat cycle applied to the original JET components and the one followed at IC for the specimens to be tested. The differences between the two treatments are mainly due to dissimilar equipment used each time. The original treatment was carried out in large vacuum ovens (necessary for the subsequent brazing of the pipework), while the IC cycle was performed by two separate ovens at atmospheric pressure. The solution treatment was carried out in the first oven, which was programmable and therefore able to perform pre-set temperature variations versus time, but incapable of rapid quenches. An additional oven (set at 475°C) was used for the aged-hardening phase. The temperature during the heat treatment was continuously monitored not only by the oven sensors but also by additional thermocouples attached to the specimens.

The exposure of the hot samples to air caused significant oxidisation. Black and red areas became visible on the sample surfaces, indicative of the formation of both copper oxides, CuO (cupric oxide) and $Cu_2O$ (cuprous oxide) respectively. At temperatures higher than 200°C [11] (as during the final quench phase), the oxide films start to exfoliate (flake off), thus continually re-exposing the underlying metal to further oxidation till cooling down below 200°C, where they remain adherent to the main material. All specimens were polished prior to any further testing to eliminate all presence of oxides.

## 4. ROOM TEMPERATURE TESTS

### 4.1 Tensile Tests

The tensile tests were performed using a MAYES electro-mechanical screw-driven testing machine with a 200 kN load cell. The elastic displacement was measured by either an external extensometer (working range 1 mm, resolution 0.05 %, 41 mm gauge length) or strain gauges (6 mm long) attached to the samples prior to assembly into the wedge grips. Close to yield point, the displacement was recorded by switching to the MAYES internal extensometer (resolution 0.2 %, 114 mm gauge length). Each test was performed at a cross head speed of 2 mm/min and a load-displacement graph was recorded automatically throughout the test. For the room temperature tests both precipitation-hardened and solution heat-treated (as delivered) specimens were examined to quantify the effect of the heat cycle.

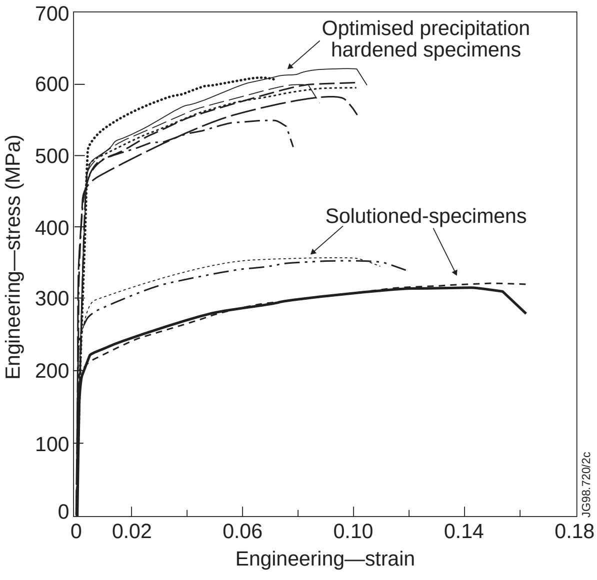


*Fig.5. Stress Strain curves obtained from room temperature tensile tests of solution and precipitation hardened CuNiSi specimens.*

Fig. 5 shows the engineering stress-engineering strain curves as derived from the respective load-displacement measurements from a series of tests at room temperature. The lower four curves represent the as supplied specimens while the others show the additionally treated specimens. It may be seen that the optimised heat treatment process has produced a material with almost double yield, tensile and rupture strength, (mean values of 430, 593 and 575 MPa respectively, with a variation of ±20 MPa) and reduced ductility. The Young's Modulus was not affected by the heat process and it was found to be 125 ±1 GPa.

The CuNiSi showed little strain hardening and significant ductility. In general, the shape of the curves obtained are similar to those found in the literature concerning CuNiSi with similar heat treatments, e.g. [12]. The reproducibility of the precipitation hardened specimens, with which the present work is primarily concerned (since they represent the real components), is good. However, there is a noticeable spread after yielding, that is more or less similar for both the solution treated (ie, as received) and precipitation hardened samples, though the former seem to occupy the extreme upper and lower band of the scatter (due to the smaller number of specimens used in this case). The as supplied samples showed a yield, tensile and rupture strength of 226±33, 339±22 and 320±30 MPa respectively. The spread cannot be attributed to orientation effects, since the specimens were cut in the same direction and they were also examined afterwards by microscope. It may be caused due to localised effects during the manufacturing process or due to inaccuracies in the machining process.

Another important aspect was the fracture mode of the specimens. The solution treated specimens displayed a very ductile behaviour with a significant reduction of area (88%) and necking of the specimen (see Fig. 6) while the precipitated ones showed a more brittle fracture, with low necking and lower reduction of area (15%). Fig 6 illustrates the two very different appearances of the fracture surfaces. The dimpled rupture of the solution-treated samples occurred on a plane $90^o$ to the axis of the tensile load, while the brittle specimens failed at an angle approximately $45^o$ to the tensile axis.

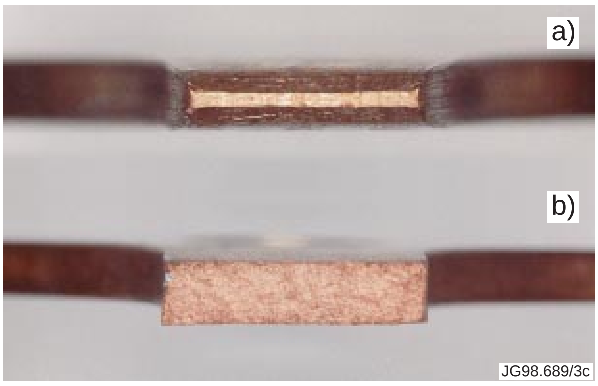


*Fig.6. Fracture surface of a) solution and b) precipitation hardened CuNiSi specimens following a room temperature tensile loading.*

**4.2 Fracture toughness tests.**

Only precipitation-hardened CT specimens were used for the fracture toughness tests. The relatively limited thickness of 3 mm and the high ductility of the material shown in the tensile tests suggested that a $K_{IC}$ test might prove inappropriate.

The CT-specimens were milled initially with a blunted notch (27 mm long and 1.3 mm wide, see Fig 3) that was subsequently cut to a V-shape sharp edge by a special saw blade. A valid fracture toughness test requires the specimens to be precracked in fatigue, a necessary step for introducing a crack of physical size. Following the heat treatment, each specimen was attached to a servo-hydraulic testing machine and subjected to a cyclic-loading with 27 Hz frequency from a 5 kN load cell. Before the tests, preliminary runs were made to check alignment and performance. The crack propagation, of up to 2 mm from the machined notch, (the minimum requirement was 1.3 mm for the specimen dimensions [9]) was monitored by an optical microscope (×35 magnification) clamped to the testing machine, and was achieved after about $70\times10^3$ cycles on average.

The precracked specimens were then tested statically in an Instron servohydraulic testing machine with a 20 kN load cell at room temperature. The load-line displacement curves, shown in Fig. 7, were recorded digitally (after converting the analogue signals); data were stored and manipulated by a 486-Microprocessor PC. The reproducibility of the results is good; the lower curve seems to divert initially from the "average" material behaviour, due to some grip slippage suspected to have occured at the beginning of the test, and indicated by the abrupt slope change of the curve at low displacements. The force-displacement curves were examined in accordance with the specifications laid in the standards [10] for a valid $K_{IC}$ test. It was found that both criteria (ie, $v_1<0.25$ v and $P_{max}/P_Q< 1.1$) were not satisfied due to the high non-linearity of the curves, suggesting that the retrieved data were inappropriate for a valid $K_{IC}$ test, as was anticipated. Therefore $J_{IC}$ tests were carried out to determine the fracture toughness.

The multiple specimen technique was adopted for the $J_{IC}$ test. To obtain a valid property value, a number of $J$ and corresponding crack growth ($\Delta$a) values are required, with at least four data within specified limits of crack growth. The first specimen was loaded to failure (i.e. curve 1, Fig 7) and from then onwards the rest of the samples were subjected to loads close to the maximum values, either prior to or after the peak load value. At that point, the load was removed.

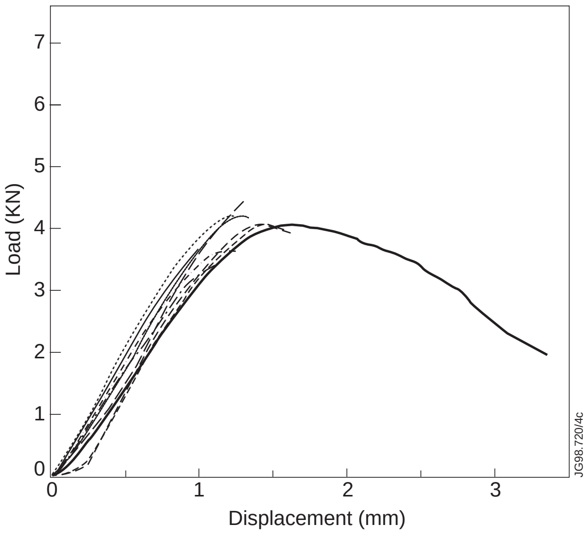

*Fig.7. Experimental Load-Displacement traces, as recorded during room temperature fracture toughness tests with CT CuNiSi specimens.*

To identify the amount of crack growth, the specimens were placed in a hot oven (480°C) to be oxidised, then removed and submerged in LN and immediately afterwards broken open at the Instron machine. The fracture surface produced during the axial tensile loading, shown in Fig. 8, exhibits the characteristic triangle-shape, demonstrated also in thin samples of Aluminium alloy [13], indicating that even thin specimens exhibit a tunnelling effect. There was some consideration as to which length is more representative of the real crack growth. An engineering approach was adopted in this case, whereby $\Delta$a was taken as half the height of the triangular shaped fracture surface. The


*Fig.8. Characteristic triangular shape of a CT fractured surface demonstrated throughout the fracture toughness tests at all temperatures.*

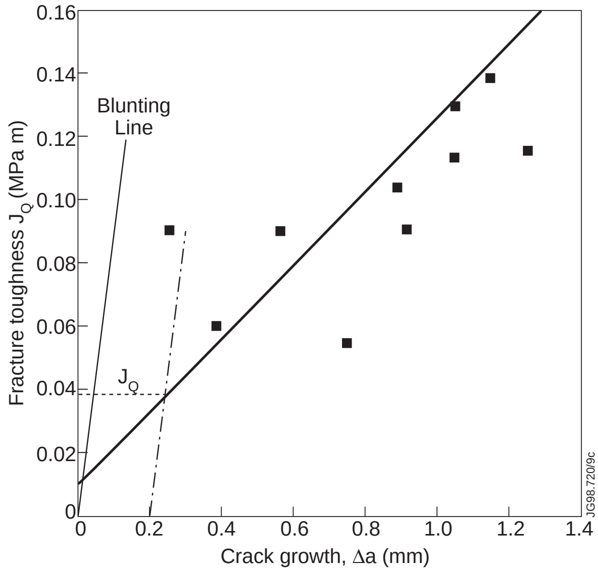


*Fig.9. Measured* J *versus crack extension, Δa, from a series of room temperature fracture toughness tests with CT CuNiSi specimens. Δa assumed as half the height of the triangular fractured surface.*

standards consider the crack extension as the average value of seven measurements across the thickness, but for the relatively thin specimens (3 mm) this was impractical. $J$ values were evaluated from the area of the load-displacement record after integration with suitable software [14]. The results of the $J_Q$ versus crack growth, Δa, are shown in Fig. 9. According to [9], the data used to obtain $J_{IC}$ should satisfy certain requirements. At least four data points must remain within the valid region enclosed by exclusion lines. It can be seen in Fig. 9 that indeed four points (the minimum requirement) lie in the valid region but quite a lot of measurements are outside the 1.5 mm exclusion line, due to the relatively large amounts of crack growth. A linear regression line based on the least square-method was fitted on the valid data and $J_Q$ was found to be ~0.038 MPa m.

## 5. LOW TEMPERATURE TESTS

The Siclanic LN screens of the JET cryopump operate mainly at $-196^{o}$C, and thus it was imperative to define its properties at LN temperatures. Tests were performed at two different temperatures, $-80^{o}$C and $-196^{o}$C.

### 5.1 Tensile Tests at $-80^{o}$C.

The temperature, of $-80^{o}$C, was achieved by using the boil off from a LN dewar. The specimens to be tested were enclosed in a rectangular metallic chamber bolted on the Instron testing machine and connected to the LN dewar by a flexible hose. The dewar supply valve was operated by a temperature controller through a sensor placed at the inner side of back chamber wall. The set point of the controller was $-100^{o}$C. Due to heat conduction from the surroundings, the specimen temperature was higher than the set point, and the former was being recorded continuously throughout the tests by a separate thermocouple. Strain gauges, of the CFLA-6.350-II type, 6 mm long, (TML Japan) and capable to withstand cryogenic temperatures, were attached with a special adhesive (EA-2, TML Japan) to the samples prior to assembly. The data from the 20 kN load cell and extensometer of the testing machine were retrieved directly by a PC and stored for further manipulation. The results of the tensile tests are shown in Fig. 10. The mean values of the yield, tensile and ultimate strength were found to be 425 ±10, 600±30 and 555±10 MPa respectively, which do not differ much from the tensile tests at room temperature, suggesting that the effect of temperature at this level is negligible. The ductility is similar in both temperatures with a total strain of 0.1.

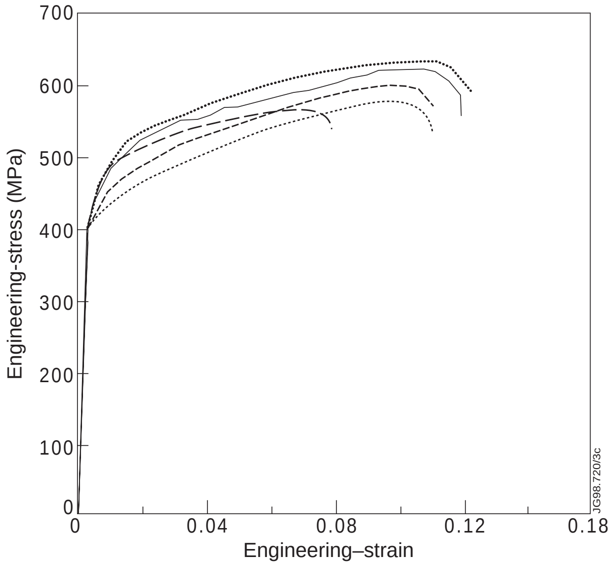


*Fig.10. Stress-Strain curves obtained from tensile tests of precipitation hardened CuNiSi specimens, performed at -80$^o$C by means of cold gaseous Nitrogen.*

**5.2. Fracture Tests at –80$^o$C**

The same configuration for the Instron machine was used for the fracture toughness tests of CT specimens at –80$^o$C. The load-line displacement of ten such tests are shown in Fig. 11. It appears that there is not much difference to the test carried out at room temperature (Fig. 7) which indicates that the CuNiSi does not become brittle at this temperature. This is also supported by Fig. 12, which shows $J_Q$ plotted against crack growth, Δa. The points which lay inside the valid area are again four (the minimum requirement) while the rest are disregarded. The resultant $J_Q$ was found to be higher than before, at a value of ~0.105 MPa m. The fracture surface of the specimens was similar to the room temperature one showing again the characteristic triangle-shape of the crack area. However, the scatter in the test is much more noticeable than before. It is highly unlikely to be due to orientation effects, since only TL or LT specimens could have been cut, types which are known not to cause significant differences on the results [15].

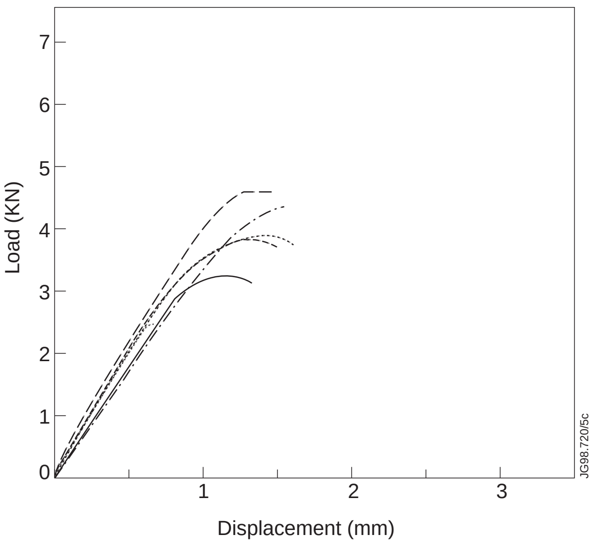


*Fig.11. Load-Displacement traces obtained during fracture toughness tests at -80°C with CT precipitation hardened CuNiSi specimens.*

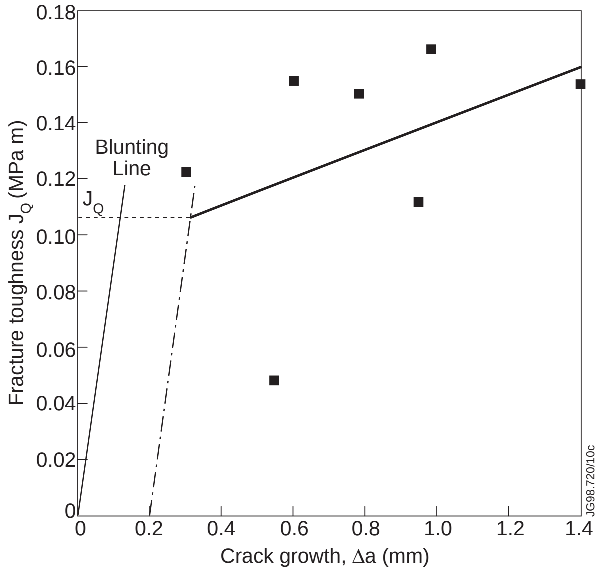


*Fig.12. Measured* J *versus crack extension, Δa, from a series of fracture toughness tests at -80°C with CT precipitation hardened CuNiSi specimens. Δa assumed as half the height of the triangular fractured surface.*

### 5.3 Fracture Toughness tests at −196°C.

Only fracture toughness tests were carried out at this temperature. Tensile data were taken from the two measurements carried out by Riso [16], which showed yield of 459±3 MPa, tensile of 543±2 MPa and rupture of 475±5 MPa.

A special stainless steel cylindrical chamber was designed and constructed at JET. The chamber had an open top end, while the rest of its exterior surfaces were covered by thermal insulation to minimise heat losses. Its base was screwed to a threaded bottom shackle, deforming at the same time plastically a conical aluminium seal incorporated in the assembly for a leak tight configuration. After attaching a specimen to the testing machine inside the chamber, LN was poured in till both specimen and shackles were fully submerged. Load was not applied until thermal equilibrium was reached (i.e. till boiling ceased).

Load line displacement and the calculated *J*-integral versus crack growth are shown in Figs 13, 14 respectively. It can be seen that all but two points can be regarded as valid while the value of $J_{IC}$ was found to be ~0.4 MPa m, which is higher by a factor of ~3.7 than the results obtained with tests using GN cooling (i.e. -80°C).

Fig 15 illustrates the effect of temperature on the tensile, yield, rupture strength, as well as on the fracture toughness of Siclanic. It appears that the temperature does not affect significantly the strength values. However, a slight increase of yield strength with decreasing temperature can be detected as opposed to the reverse behaviour of the ultimate and rupture strength. This tendency is not pronounced and can be counter argued in view of the existing error bands. In contrast, the fracture toughness seems to increase at cryogenic temperatures. Similar trends are

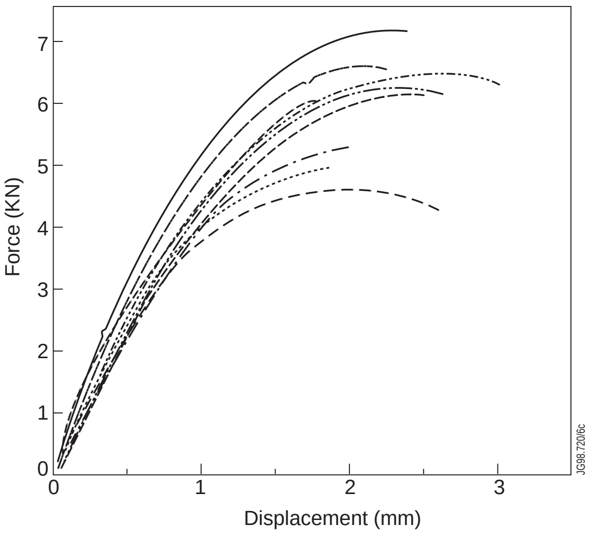


Fig.13. Load-Displacement traces obtained during fracture toughness tests at -196°C with CT precipitation hardened CuNiSi specimens.

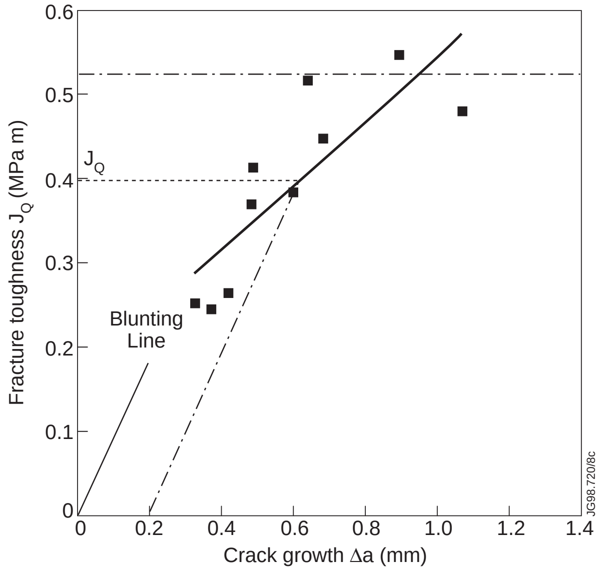


Fig.14. Measured J versus crack extension, Δa, from a series of fracture toughness tests at -196°C with CT precipitation hardened CuNiSi specimens. Δa assumed as half the height of the triangular fractured surface.

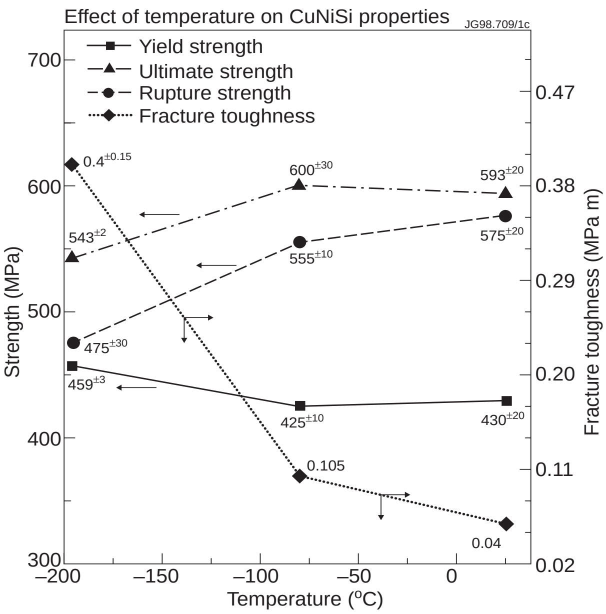


Fig.15. Effect of Temperature on the strength and fracture toughness of precipitation hardened CuNiSi.

quoted in the literature[15] for the fracture toughness of annealed fcc alloys which usually can increase by up to 175%, between 25°C and -269°C, often showing a broad maximum at -196°C. For precipitation hardened alloys however (which are of relevance here) the change in fracture toughness is moderate, by an average of ±30%.

## 6. FRACTOGRAPHY

A Scanning Electron Microscope (SEM) was used at IC to analyse the fracture surfaces of the specimens. Figure 16 depicts the surface of the solution (as received) and precipitation hardened

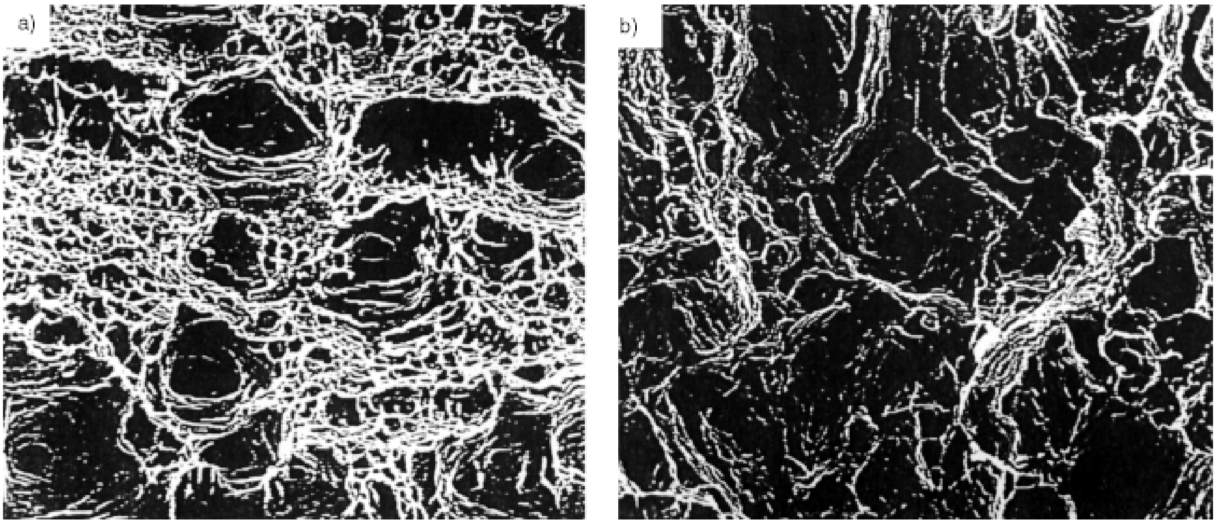


*Fig.16. Scanning Electron Fractographs of a) solution and b) precipitation hardened CuNiSi samples fractured by tensile loading at room temperature.*

specimens fractured during a tensile loading at room temperature. In both cases, the material exhibits high ductility. However, the fracture type of the solutioned material is characterised by a ductile microvoid coalescence exhibiting three distinct void sizes, perhaps associated with three different nickel silicides formed during the corresponding dwell stages of the heat treatment

Figure 17 shows a number of typical images of a tensile specimen fractured at $-80^{o}$C (Fig 17a) and CT specimens fractured at room temperature (Fig 17b) and $-80^{o}$C (Fig 17c) respectively, following a fracture toughness test. The type of fracture still falls in the category of dimple rupture but as far as the crack path is concerned there is a mixture of intergranular and transgranular cracking. Copper and its alloys being materials with a face centred cubic (f.c.c.) lattice do not normally exhibit fracture by cleavage.

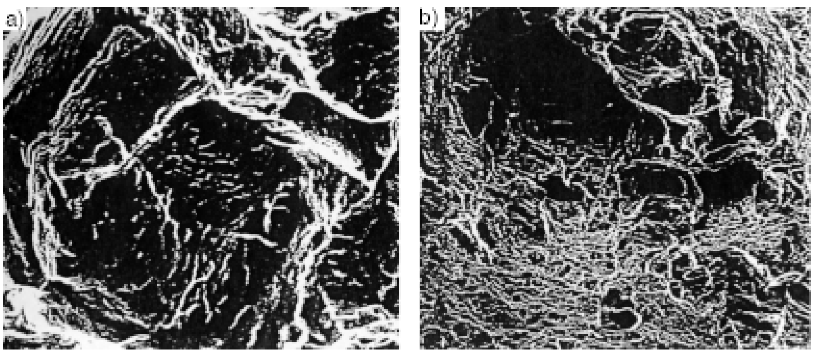


*Fig.17. Typical Scanning Electron Fractographs of precipitation hardened CuNiCi specimens fractured: (a) by tensile loading at -80$^{o}$C, (b), (c), (d) during a fracture toughness CT test at 25$^{o}$C, -80$^{o}$C.*

Images were also taken from fractured surfaces of CT specimens tested at -196$^{o}$C. However, due to a comparatively thick oxide layer formed during the heat tint phase the resultant imaging is not representative. Presently, an attempt is being undertaken to remove mechanically the oxide layer for further analysis. However, the type of fracture is expected to be similar as the one described earlier.

A further investigation with the SEM concerning the fatigue region of the CT specimens, showed no striations at any magnification, indicating that unlike some materials (eg Al) Siclanic perhaps does not have multiple slip plane systems and crack grows over specific directions.

## 7. DISCUSSION

A second stage of validation concerns the points in the valid area which should comply with the following requirements; $B > 25\ J_Q/\sigma_y$, $b_o > 25\ J_Q/\sigma_y$, with B and $b_o$ denoting the width and ligament of the specimens (see Fig. 4). The second requirement was satisfied but the specimens failed the first, because of their relatively small thickness. Nevertheless, the derived $J_Q$ can represent the behaviour of the real components of concern since they have the same thickness and may be considered to be a measure of the fracture toughness $J_c$ corresponding to this particular toughness. The true value of $J_{IC}$ is expected to be lower than this.

The assumption of a crack extension being half the height of the resultant triangular fracture surface (aiming to investigate an "average" material behaviour, as close as possible), has the following effects, if compared to a $\Delta a$ of twice the value (ie $\Delta a$ equal to the triangle height). For the room and -80$^o$C tests, all measured data with $\Delta a$ as adopted in this work, comply fully with the space requirements imposed by the relevant standards. However, for the -196$^o$C tests one datum falls beyond the plastic collapse limit, while no data are found in the acceptable region "A", as defined in the standard. In contrast, if double crack growth is assumed instead, the standard requirements are satisfied in all cases, though some of the the data have to be rejected for the two higher temperature test cases. Most importantly though is the impact on the resultant $J_Q$. If only the valid (according to the relevant standards) data are used, the difference on the $J_Q$ becomes; 16% lower and 8% higher, for the 25$^o$C and -80$^o$C tests respectively, should half crack growths be assumed. This variation turns out to be significant in case of the -196$^o$C tests, whereby $J_Q$ becomes 0.1 MPa m (assuming double crack growth) instead of 0.4 MPa m, indicating at the same time at most a moderate effect of temperature on the fracture toughness of the material.

The evaluation of the fracture toughness through the $J(\Delta a)$ curves alone, is based broadly on macroscopic criteria- though adequate enough, since the terms, up to the fourth order, of the asymptotic series which express the stress strain field close to the crack tip and fracture process zone, and for plane stress conditions are all controlled by a single parameter, $J$ (or CTOD) [17]. This approach does not necessitate any microscopic understanding of the fracture events involved [18]. The latter however was dealt partly with the fractographic analyses which have shed some light on the fracture mode, that was found to be predominately of a microvoid coalescence type. The crack growth curves, obtained in this work, do not demonstrate clearly the crack initiation limit (defined as the intersection between the blunting line and the crack growth curve).

For a more accurate evaluation of $J_{IC}$ it would be possible to employ a stress modified critical strain criterion, presented initially in [19-22] which is complimentary to the critical crack tip opening displacement (CTOD) method [18, 23-25]. The former is formulated as: $J \sim \sigma_o \bar{\varepsilon}_f^* l_o^*$ where $\bar{\varepsilon}_f^*$ denotes the fracture strain or ductility, specific to the relevant stress rate over a characteristic distance $l_o$* which in turn denotes the mean void initiating particle spacing. Further work is needed to incorporate such an analysis, since $\bar{\varepsilon}_f^*$ is not equated to either the tensile (or plane strain) ductilities measured conventionally [18].

## 8. CONCLUSIONS

Data have been presented for the tensile and fracture behaviour of thin plate Siclanic. It has been found that the yield strength of the material is relatively insensitive to temperature and the fracture toughness showing an apparent increase in toughness with reducing temperature.


## ACKNOWLEDGEMENTS

The authors wish to thank the JET Joint Undertaking for supporting this project and especially Dr D Stork and Mr M Watson for their continuous interest. Acknowledgements are due to all the technical staff at Imperial College, and in particular, Mr H McGillivray, Mr A Noorbai, Mr N Taylor, and Mr P Savage, as well as to Mr Peter Webster from the Copper Development Association, UK, Mr Polve Brondsted from the Materials Research Department, Riso Netherlands and Dr Baker at Imperial College.


## REFERENCES


[1] MSX-BL and CLAL. Siclanics: Conductive Alloy for Contact Blades, Data sheet U 102E/244, France.

[2] Handbook of Materials for Superconductive Machinery; MCIC-HB-04, Advanced Research Project Agency &Cryogenics Division, National Bureau of Standards, USA 1974.

[3] G J Butterworth & C B A Forty: A survey of the properties of copper alloys for use as fusion reactor materials. Review article, Journal of Nuclear Materials, Vol. 189, pp 237-276, North Holand, 1992

[4] V Johnson. Properties of Materials at low Temperature. A Compendium. National Bureau of Standards, Cryogenic engineering Laboratory, 1961, Part 2, Chapt 3, Pergamon Press USA.

[5] Copper Development Association, CDA, Copper and Copper Alloy Data, Datat Sheet: F1-F3, G1-G6, H1-H7, K1-K7, L1-L5, M1-M2, Editions 1971-1973.

[6] S. Papastergiou, W. Obert and E. Thompson: Materials Selection, Qualification and Manufacturing of the In-Vessel Divertor Cryopump for JET, Advances in Cryogenic Engineering, Vol. 40, pp1429-1436, Plenum Press, 1994.

[7] BS 2870: Specifications for Rolled Copper and Copper alloys : sheet , strip and foil, British Standards Institution, 1980.

[8] Methods for Tensile Testing of Metals: British Standard 18, Part 3, 1971.

[9] A Measure of Fracture Toughness: Standard Test Method for $J_{IC}$, ASTM Standard, Designation E 813-89, American Society for Testing and Materials ,1989.

[10] Standard Test Method for Plain Fracture Toughness of Metallic Materials: ASTM Designation E 399-90, American Society for Testing and Materials, 1990.

[11] Copper Data, Copper Development Association (CDA) Technical Note TN20, April 1975.

[12] R Reed & R P Mikesell: Low temperature Mechanical Properties of Copper and Selected Copper Alloys, National Bureau of Standards Monograph 101, USA, 1967

[13] D Broek: The Practical Use of Fracture Mechanics, Sec. 5, Kluwer academic Publishers, 1989, Netherlands.

[14] ORIGIN Ver 5.0, 1998, MicroCal Software, Inc, Northampton, MA 01060 USA.

[15] R P Reed & A F Clark: Materials at low Temperature, National Bureau of Standards, American Society of Metals, USA, 1983.

[16] Riso National Laboratory, Materials Department: Report on Heat Treatment and Measurements of Mechanical Properties of CuCrZr and CuSi Alloys, Contract No 02054-00, Denmark, December 1990.

[17] Yuh-Jin Chao. On a single Parameter Controlled Fracture of Solids under Plane Stress Conditions, Intern. Journal of Fracture, 1993, Vol. 62, 7-10, Kluwer Acaddemic Publishers, Netherlands.

[18] R. O. Ritchie & A W Thompson. On Macroscopic and Microscopic Analyses for Crack Initiation and Crack Growth Toughness in Ductile Alloys. Matallurgical Transactions A, 1985, 16A, 236-248.

[19] F A McClintock. Journal of Applied Mechanics. ASME Transactions, Series E 1968, Vol. 35, 363-71

[20] A C Mackenzie, J W Hancock & D K Brown. Eng. Of Fracture Mechanics, 1977, Vol. 9, pp 167-88

[21] R C Bates: in Metallurgical Treatises, 1982, 551-70, TMS-AIME Warrendale

[22] R O Ritchie W L Server & R A Wullaert. Metall. Transactions A 1979, Vol. 10A, 1557-70.

[23] F A McClintock. In Physics of Strength and Plasticity. 1969, 307-26, A S Argon MIT Press , Cambridge, MA USA.

[24] J R Rice & M A Johnson. In Inelastic Behaviour of Solids, 1970, 641-72, McGraw Hill, New York.

[25] J R Rice & D M Tracey. Journal of Mech. Phys. Solids, 1969, Vol. 17, 201-17.